GEOPHYSICAL RESEARCH LETTERS, VOL. 34, L07303, doi:10.1029/2007GL029189, 2007

Stress before and after the 2002 Denali fault earthquake

Robert L. Wesson[1] and Oliver S. Boyd[1]

Received 15 January 2007; revised 26 February 2007; accepted 6 March 2007; published 10 April 2007.

[1] Spatially averaged, absolute deviatoric stress tensors along the faults ruptured during the 2002 Denali fault earthquake, both before and after the event, are derived, using a new method, from estimates of the orientations of the principal stresses and the stress change associated with the earthquake. Stresses are estimated in three regions along the Denali fault, one of which also includes the Susitna Glacier fault, and one region along the Totschunda fault. Estimates of the spatially averaged shear stress before the earthquake resolved onto the faults that ruptured during the event range from near 1 MPa to near 4 MPa. Shear stresses estimated along the faults in all these regions after the event are near zero (0 ± 1 MPa). These results suggest that deviatoric stresses averaged over a few tens of km along strike are low, and that the stress drop during the earthquake was complete or nearly so. **Citation:** Wesson, R. L., and O. S. Boyd (2007), Stress before and after the 2002 Denali fault earthquake, *Geophys. Res. Lett.*, *34*, L07303, doi:10.1029/2007GL029189.

1. Introduction

[2] While analysis of earthquake focal mechanisms permits the determination of the orientation of the principal stresses at seismogenic depths in the Earth's crust, estimation of the magnitude of the shear stress acting on faults at these depths prior to earthquake rupture remains the subject of controversy. Issues include laboratory measurements of the static frictional strength of rocks and fault zone materials that suggest strengths (at about 5 km depth and in the absence of abnormal fluid pressures) of about 50 MPa, seismological and geodetic observations that suggest typical stress drops observed during moderate to large earthquakes of about 0.1 to 10 MPa, and the constraint indicated by the lack of an observed heat flow anomaly that indicates an upper bound on the shear stress of about 20 MPa. See *d'Alessio et al.* [2006] and *Scholz and Hanks* [2004] for recent reviews.

[3] In this paper we present a new method that enables estimates of the spatially averaged, absolute deviatoric stress resolved on the Denali, Susitna Glacier and Totschunda faults both before and after the 2002 Denali fault earthquake (Mw 7.9). The Denali fault earthquake began with thrust and right lateral slip on the Susitna Glacier fault (a thrust fault dipping northward and intersecting the Denali fault at a depth of about 6 km), then continued as a primarily right lateral strike-slip event for a total distance of about 300 km along the Denali and Totschunda faults [*Haeussler et al.*, 2004]. Average slip was about 4 m [*Haeussler et al.*, 2004; *Hreinsdóttir et al.*, 2006]. Maximum slip is estimated in the range 8–10 m.

[4] We combine the results from seismologic studies indicating the orientation of the principal stresses before and after the earthquake (inferred from the focal mechanisms of small earthquakes within about 30 km of the Denali fault), together with the stress change in the Earth's crust inferred from the slip models determined through the inversion of geodetic and geologic data, to estimate the deviatoric stresses acting on the fault before and after the event. The resulting estimates are not of peak stresses along the fault, but rather estimates of the stress averaged or smoothed over length scales of a few tens of kilometers parallel to the fault and a few km perpendicular to the fault.

2. Observations: The Denali Fault Earthquake

[5] In four regions along the rupture of the Denali fault earthquake we consider the stress orientations before and after the event, together with an estimate of the average stress change derived from a slip model of the earthquake (Figure 1). Region O1 includes the hypocenter of the mainshock and the Susitna Glacier fault. Region O2 includes the central part of the rupture, the Richardson Highway and TransAlaska Pipeline fault crossing. Region O3 includes the eastern portion of the fault rupture along the Denali fault with the largest values of displacement. Region O4 includes the portion of the rupture along the Totschunda fault.

[6] *Ratchkovski* [2003] and *Ratchkovski et al.* [2004] reported large rotations of the principal stresses at the time of the Denali fault earthquake, with clockwise rotation ranging from about 14° in the western part of the rupture to as much as 38° in the eastern part. Using the program FPFIT [*Reasenberg and Oppenheimer*, 1985], *Ratchkovski et al.* [2004] determined focal mechanisms for earthquakes before and after the Denali fault earthquake, then estimated the orientations of the principal stresses using the ZMAP implementation [*Weimer*, 2001] of the stress-tensor inversion method of *Michael* [1984, 1987]. Also following the event, there was an increased tendency for thrust mechanisms along portions of the rupture, as contrasted with strike-slip prior to the event, indicating that the least compression had changed from horizontal to vertical.

[7] We use the focal mechanisms determined by *Ratchkovski et al.* [2004], subdivided into slightly different regions. Before the Denali fault earthquake (and after the M6.4 Nenana Mountain earthquake in October of 2002 for region O1), we have 10, 26, 6, and 6 focal mechanisms for regions O1, O2, O3 and O4. The corresponding numbers after the earthquake are 53, 45, 41, and 19. The pressure and tension axes as well as the orientations of the principal axes determined by *Michael*'s [1987] method are shown in Figure 2. The rotations of the principal compression, S1, are about 9°, 15°, 35°, and 32° clockwise for the regions O1

[1]U.S. Geological Survey, Golden, Colorado, USA.

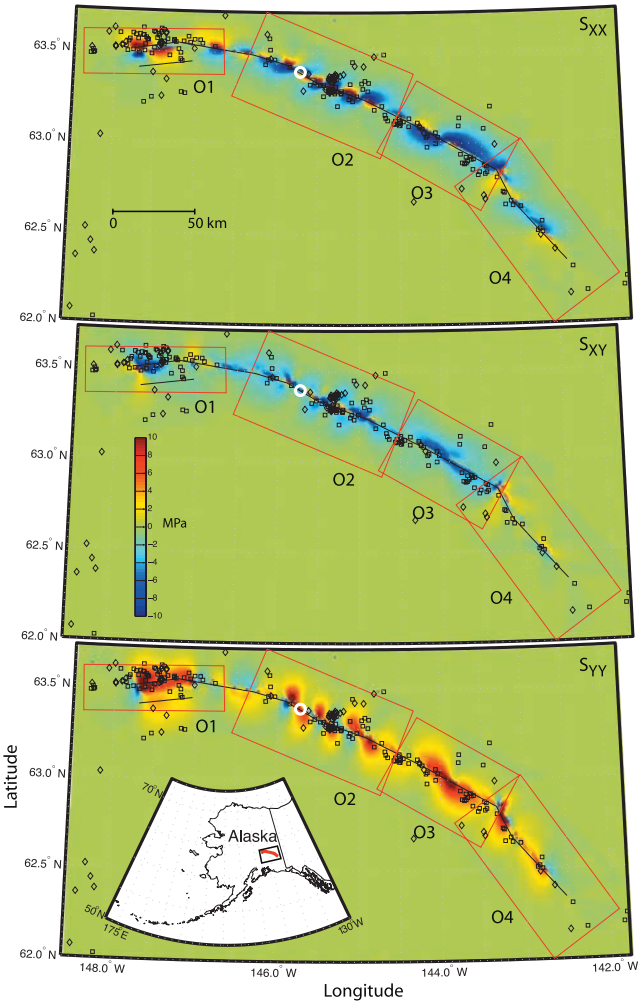

Figure 1. Denali fault and surrounding area showing surface ruptures associated with the 2002 earthquake and outlines of subregions. The three panels show the calculated change in the S_{xx}, S_{xy}, S_{yy} components of the stress tensor from the resampled dislocation model of *Hreinsdóttir et al.* [2006]. The stress changes were averaged at the locations of the aftershocks shown by the open squares. Locations of earthquakes occurring before the Denali rupture appear as open diamonds. All six components of the stress tensor were considered in the analysis but are not shown here. White circle shows location of Richardson Highway and TransAlaska Pipeline crossing of the fault. Inset in bottom panel shows location of surface ruptures of Denali fault during the earthquake (red line).

through O4 respectively, in close agreement with *Ratchkovski et al.* [2004]. In regions O2, O3 and O4, the intermediate stress, S2, is near vertical prior to the earthquake, while the least compression, S3, is near vertical after.

[8] From the observed displacement of GPS sites in Alaska and Canada, and the observed geologic surface offsets, *Hreinsdóttir et al.* [2006] estimated coseismic fault displacements in a detailed dislocation model of the rupture along the Susitna Glacier, Denali and Totschunda faults, predominately right-lateral along the Denali and Totschunda faults with a significant component of north-side up displacement along the Denali and Susitna Glacier faults. Inferred slips locally reached 8 m or more along the eastern two-thirds of the rupture. Slip on the Susitna Glacier fault also reached a maximum of about 8 m.

[9] *Hreinsdóttir et al.* [2006] specified their slip model on a set of rectangular dislocations each 3 km × 3 km, vertical along the Denali and Totschunda faults, and dipping northward along the Susitna Glacier fault. The model extends 303 km horizontally and to a depth of 18 km.

[10] From this slip model, we estimate the stress change associated with the earthquake at a depth of 5 km using the computer code 3D-DEF [*Gomberg and Ellis*, 1993, 1994] based on the equations of *Okada* [1992]. We assume a Poisson's ratio of 0.28 and Young's modulus of 70 GPa as appropriate for this depth. To minimize numerical artifacts, we resampled the Hreinsdóttir model, interpolating (and extrapolating at the edges) to yield a dislocation model composed of dislocation tiles 0.3 km wide by 0.21 km high. The resampled model should be nearly identical to the original model from the point of view of the predicted displacements of GPS monuments and geologic surface displacements, and while it does not eliminate artifacts introduced by the assumption of constant slip on each dislocation tile, it significantly moderates their influence. Three components of the calculated stress change are shown in Figure 1.

3. Estimating the Magnitudes of the Deviatoric Stresses

[11] *Sonder* [1990], *Zoback* [1992] and *Hardebeck and Hauksson* [2001] have given expressions in two dimensions relating the change in orientation of the principal stresses to a change in shear stress. We show here a method that can be used in three dimensions to estimate the deviatoric stress tensor before and after a large earthquake. To begin, the difference in the stress tensor before and after the earthquake is equal to the change in stress associated with the earthquake,

$$\Delta\mathbf{S} = \mathbf{S}^{after} - \mathbf{S}^{before} \tag{1}$$

where the stress change, $\Delta\mathbf{S}$, is found by averaging the stress tensors resulting from the slip model at the locations of the aftershocks. Each of these tensors can be split into its deviatoric and isotropic parts, which must satisfy equation (1) independently. Therefore for notational simplicity in the following, let all stresses be considered deviatoric unless explicitly stated otherwise. Although the stress tensor inversion method of *Michael* [1984, 1987] is commonly used to give the orientations of the principal stresses (the eigenvectors of the stress tensor), and the ratio of the differences of the principal stresses, ϕ, equivalently the method yields a normalized version of the deviatoric stress tensor. If we let the normalized deviatoric stress tensor from *Michael*'s [1984] method be $\mathbf{s}$, and the absolute deviatoric stress tensor be $\mathbf{S}$, then we can write

$$\mathbf{S}^{before} = \alpha\mathbf{s}^{before}$$

and (2)

$$\mathbf{S}^{after} = \beta\mathbf{s}^{after}$$

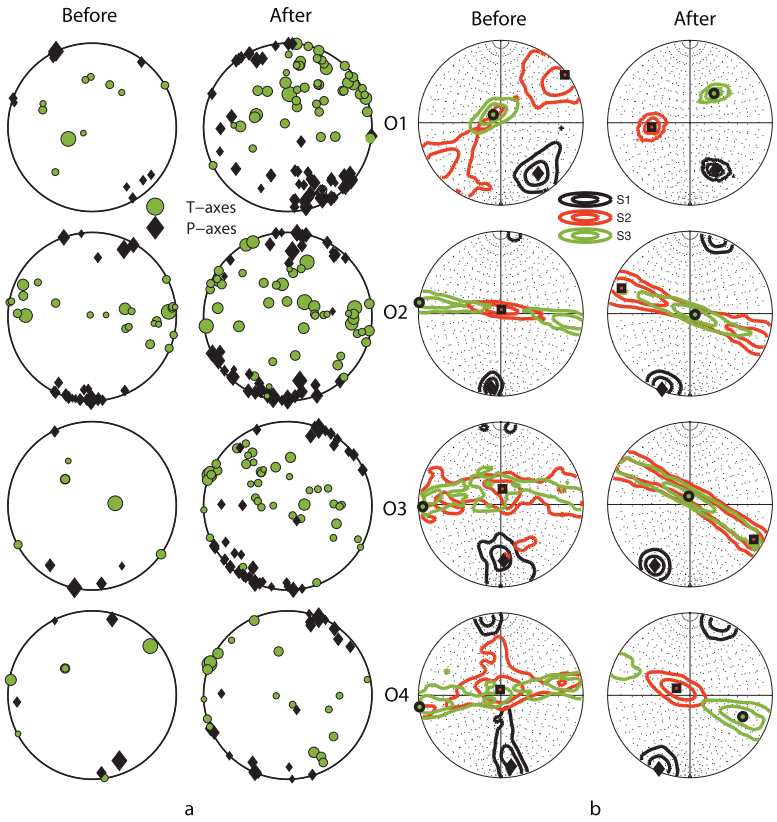

Figure 2. (a) P (black diamonds) and T (green circles) axes of focal mechanisms of *Ratchkovski et al.* [2004] used in this study. Their size is proportional to earthquake magnitude. Focal mechanisms were aggregated to estimate the average orientation of the principal stresses in subregions O1–O4 before and after the earthquake. (b) Stress orientations determined by the method of *Michael* [1984, 1987] and the program ZMAP for the three principal directions of the stress tensor, S1 (the greatest compression, in the diamonds and black contours), S2 (the intermediate stress, in the squares and red contours), and S3 (the least compression, in the circles and green contours). The contours show the 66% and 95% confidence limits as determined by the bootstrap analysis. Notice in all regions the clockwise rotation of S1, and in regions O1, O2 and O3 the swapping of the orientations of S2 and S3.

where the superscripts *before* and *after* signify stresses before and after the Denali earthquake, and α and β are the unknown scale factors that relate the normalized and absolute deviatoric stress tensors. Thus (1) can be rewritten as

$$\Delta\mathbf{S} = \beta\mathbf{s}^{after} - \alpha\mathbf{s}^{before}. \tag{3}$$

[12] Since we are dealing with deviatoric stresses (implying that $s_{zz} = -(s_{xx} + s_{yy})$), there are only five independent components. Considering the stresses in (3) as column vectors of the five independent components, we can then rewrite (3) as

$$\begin{bmatrix} \Delta S_{xx} \\ \Delta S_{xy} \\ \Delta S_{xz} \\ \Delta S_{yy} \\ \Delta S_{yz} \end{bmatrix} = \begin{bmatrix} s_{xx}^{after} & -s_{xx}^{before} \\ s_{xy}^{after} & -s_{xy}^{before} \\ s_{xz}^{after} & -s_{xz}^{before} \\ s_{yy}^{after} & -s_{yy}^{before} \\ s_{yz}^{after} & -s_{yz}^{before} \end{bmatrix} \begin{bmatrix} \beta \\ \alpha \end{bmatrix}. \tag{4}$$

We can find a linear least squares solution for α and β that minimizes the norm of the difference vector between the right- and left-hand sides. Since to consider negative values of α and β would be equivalent to reversing the sign of the stress difference and thus violating the observations of stress orientation, we constrain α and β to be positive and use the non-negative least squares method of *Lawson and Hanson* [1974]. Inserting α and β back into (2), we produce estimates of the absolute deviatoric stress tensors before and after the event. Resolved shear stresses on the faults calculated using all the focal mechanisms within each region are shown in Table 1 in the columns marked "All data." The right-lateral shear stresses range from 0.9 to 3.8 MPa prior to the earthquake, and from 0.0 to 0.4 MPa after.

4. Analysis of Uncertainties

[13] Obviously there are a number of uncertainties in the above analysis. The sources of uncertainty include 1) uncertainty in the principal stress directions inferred from the focal mechanisms, 2) uncertainty in the change in stress (related to the uncertainty in the slip model and the sampling and smoothing of the change in stress), and 3) uncertainty related to the less than perfect fit of α and β during the least squares inversion. We will examine the effect of uncertainties in the slip model more formally in future work, but we examine here the influence of the other factors on the final result. We anticipate that the large

Table 1. Shear Stresses (MPa) Resolved on Principal Faults and Scale Factors, α and β, Before and After the Event[a]

	Before								After							
	Strike-Slip			Dip-Slip			Alpha		Strike-Slip			Dip-Slip			Beta	
		Bootstrap			Bootstrap		Bootstrap			Bootstrap			Bootstrap		Bootstrap	
Fault	All Data	Mean	S.D.	All Data	Mean	S.D.	Mean	S.D.	All Data	Mean	S.D.	All Data	Mean	S.D.	Mean	S.D.
Western Denali	0.9	1.5	1.0	0.8	0.9	0.6	2.2	1.1	0.3	0.8	0.7	0.3	0.9	0.7	1.2	1.0
Susitna Glacier	1.0	1.3	0.8	1.4	1.9	1.0	2.2	1.1	0.2	0.4	0.4	−0.2	0.4	0.4	1.2	1.0
Central Denali	2.7	2.1	1.0	0.9	0.6	0.6	4.2	1.9	0.3	0.2	0.6	0.2	0.3	0.7	4.5	2.3
Eastern Denali	3.8	3.0	1.1	2.3	1.5	1.2	3.1	1.0	0.0	0.0	0.4	0.9	0.7	0.5	2.5	1.2
Totschunda	2.3	2.3	0.6	0.3	0.3	0.6	2.3	0.6	0.4	0.5	0.5	0.1	0.0	0.1	0.6	0.5

[a]Right-lateral and north-side up stresses are positive. "All data" indicates solutions obtained using all focal mechanisms. "Mean" and "S. D." are results only from combinations of bootstrap samples giving positive values of the constants α and β.

amount of spatial smoothing inherent in our approach will tend to moderate the influence of short-scale roughness and uncertainties in the slip model, as well as the impact of differences among various slip models inferred for the Denali fault earthquake.

[14] The ZMAP implementation of *Michael*'s [1984, 1987] algorithm provides a bootstrap analysis of the uncertainty in the orientation of the principal stresses. More specifically, 2000 random subsets of the focal mechanisms are used to derive 2000 realizations of the orientation of the principal stresses, producing a measure of uncertainty. It is straightforward to propagate this uncertainty through the solution of equations (4) above. We save each of 2000 bootstrap solutions for the stress orientations before and 2000 bootstrap solutions for the stress orientations after the earthquake. We take all possible pairs of 'before' and 'after' principal stress orientations and associated stress change averages and solve for the principal stresses and the stresses on the faults. This procedure results in a histogram (approximating a probability density function) for the derived stresses (Figure 3). We reject solutions where α and β are identically zero because, like the linear least squares solutions that result in negative values of α and β, we find these solutions to be physically unreasonable. Since we are considering only a subset of possible uncertainties it can be argued that our histograms are too narrow and standard deviations too small. The means and standard deviations derived from this analysis are presented in Table 1. The mean values are all within 0.8 MPa of the values calculated with all the data. The standard deviations range from 0.6 to 1.2 MPa before, and 0.1 to 0.7 MPa after.

[15] It should also be noted that as the misfit between the observed and predicted stress change, the left and right hand side of equation 4, respectively, increases, α and β tend toward smaller values. If instead of requiring all α and β to be positive, we reject solutions with relative residuals greater than 0.5, which effectively removes negative values of α and β, the curves in Figure 3 better approximate normal distributions. The means before the Denali earthquake increase by roughly 50% and the standard deviations are left unchanged.

[16] We prefer the mean estimates of stress from the boot strap analysis ("Mean" in Table 1), although the large standard deviations (lower bounds as discussed above) and the differences between the results for "All data" and

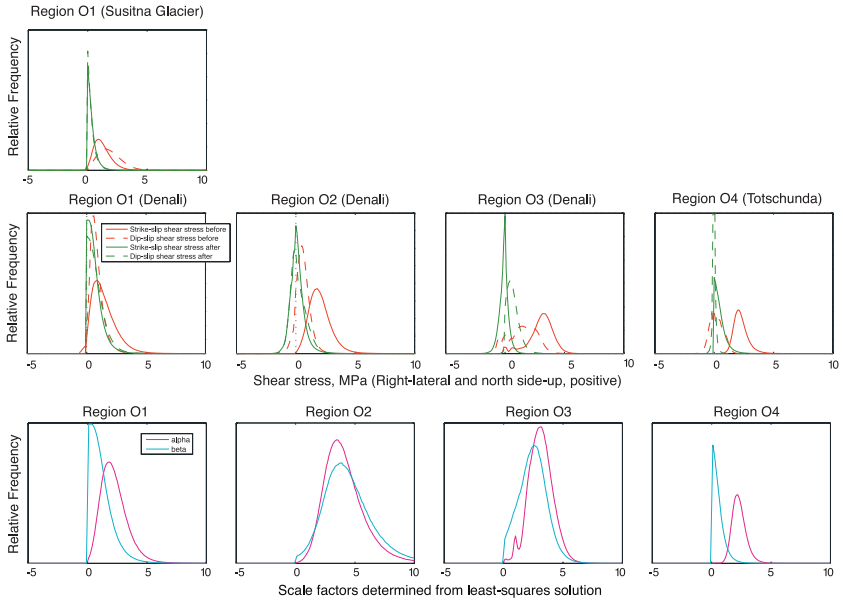

Figure 3. Histograms from bootstrap analysis for the parameters α and β and the shear stresses on the indicated faults. The solutions for α and β are required to be non-negative. Identically zero solutions for either α or β are also rejected. The number of rejected solutions depends on data quality and varies among regions.

the mean values emphasize the relatively large underlying uncertainties.

5. Discussion

[17] Results of the application of our method to the Denali fault earthquake indicate that the shear stresses resolved on the faults at a depth of 5 km, averaged over regions with dimensions 10–20 km perpendicular to the fault and of order 30–40 km parallel to the fault, are on the order of 1–4 MPa ± 1 MPa prior to the earthquake and were reduced to about 0 MPa ± 1 MPa after the earthquake. The near-complete stress drop is in agreement with the observations of *Michael et al.* [1990] and *Zoback and Beroza* [1993] following the 1989 Loma Prieta earthquake along the San Andreas fault, and *Castillo and Zoback* [1995] for the White Wolf fault following the 1953 Kern County earthquake. The region of highest average stress prior to the earthquake was located near the region of highest slip, just west of the junction of the Denali and Totschunda faults. Significant variability and peaks of higher stresses within these regions are evident, and further analysis is required to deduce how the absolute deviatoric stresses vary with spatial scale.

[18] The estimated uncertainties are a large fraction of the estimated magnitudes of the stress components. The principal contributor to this uncertainty is the relatively small number of focal mechanisms available before the event.

[19] These results seem to favor a fault that is, averaged over spatial scales of tens of kilometers, relatively weak. Assuming a normal hydrostatic gradient, coefficients of sliding friction (the ratio of shear stress to effective normal stress) at a depth of 5 km prior to the earthquake are on the order of 0.05 to 0.1.

[20] Application of the results of *Hardebeck and Hauksson* [2001, Figure 2] for two-dimensions to the geometry of the Denali fault earthquake and the stress rotations observed by *Ratchkovski et al.* [2004] confirms that the deviatoric stresses before the event should be expected to be of the same order as the stress change, as observed here. *Hardebeck and Hauksson* [2001] inferred a pre-existing deviatoric stress on the order of 10 MPa for the 1992 Landers earthquake, about two or more times the values inferred here, but also well below the values required to sustain slip if the average coefficient of friction were about 0.6.

6. Conclusions

[21] We have developed a method for estimating the magnitudes of the averaged shear and normal stresses resolved onto faults at depth in three dimensions before and after significant earthquakes together with their uncertainties. Using this method, we have derived the deviatoric stress tensors along the Denali fault before and after the 2002 Denali fault earthquake. Although the uncertainties are relatively large compared to the magnitudes of the average shear stress, the results argue strongly against average shear stresses as high as those predicted by static rock mechanics experiments assuming a normal hydrostatic gradient. In contrast, these results argue that the Denali fault is weak. The lack of appreciable shear stress on the fault subsequent to the earthquake encourages time-dependent probabilistic seismic hazard analyses.

[22] **Acknowledgments.** The authors thank Natalia Ruppert of the University of Alaska Geophysical Institute for providing her focal mechanisms and discussions, Sigrun Hreinsdóttir for providing results in advance of publication, and Jean Hardebeck, Andy Michael, Colin Williams, Bill Savage, Dave Perkins, Art Frankel, and Bill Ellsworth for helpful discussions, and two anonymous reviewers.

References

Castillo, D. A., and M. D. Zoback (1995), Systematic stress variation in the southern San Joaquin Valley and along the White Wolf fault: Implications for the rupture mechanics of the 1952 M_S 7.8 Kern County earthquake and contemporary seismicity, *J. Geophys. Res.*, *100*(B4), 6249–6264.

d'Alessio, M. A., C. F. Williams, and R. Bürgmann (2006), Frictional strength heterogeneity and surface heat flow: Implications for the strength of the creeping San Andreas fault, *J. Geophys. Res.*, *111*, B05410, doi:10.1029/2005JB003780.

Gomberg, J. S., and M. Ellis (1993), 3D-DEF: A user's manual (a three-dimensional, boundary element modeling program), *U.S. Geol. Surv. Open File Rep.*, *OFR-93-0547*, 15 pp.

Gomberg, J. S., and M. Ellis (1994), Topography and tectonics of the central New Madrid seismic zone: Results of numerical experiments using a three-dimensional boundary-element program, *J. Geophys. Res.*, *99*(B10), 20,299–20,310.

Haeussler, P. J., et al. (2004), Surface rupture and slip distribution of the Denali and Totschunda faults in the 3 November 2002 M7.9 earthquake, Alaska, *Bull. Seismol. Soc. Am.*, *94*, S23–S52.

Hardebeck, J. L., and E. Hauksson (2001), Crustal stress field in southern California and its implications for fault mechanics, *J. Geophys. Res.*, *106*(B10), 21,859–21,882.

Hreinsdóttir, S., J. T. Freymueller, R. Bürgmann, and J. Mitchell (2006), Coseismic deformation of the 2002 Denali fault earthquake: Insights from GPS measurements, *J. Geophys. Res.*, *111*, B03308, doi:10.1029/2005JB003676.

Lawson, C. L., and R. J. Hanson (1974), *Solving Least Squares Problems*, 340 pp., Prentice-Hall, Inc., Upper Saddle River, N. J.

Michael, A. J. (1984), Determination of stress from slip data: Faults and folds, *J. Geophys. Res.*, *89*(B13), 11,517–11,526.

Michael, A. J. (1987), Use of focal mechanisms to determine stress: A control study, *J. Geophys. Res.*, *92*(B1), 357–368.

Michael, A. J., W. L. Ellsworth, and D. H. Oppenheimer (1990), Coseismic stress changes induced by the 1989 Loma Prieta, California, earthquake, *Geophys. Res. Lett.*, *17*, 1441–1444.

Okada, Y. (1992), Internal deformation due to shear and tensile faults in a half-space, *Bull. Seismol. Soc. Am.*, *82*, 1018–1040.

Ratchkovski, N. A. (2003), Change in stress directions along the central Denali fault, Alaska, after the 2002 earthquake sequence, *Geophys. Res. Lett.*, *30*(19), 2017, doi:10.1029/2003GL017905.

Ratchkovski, N. A., S. Wiemer, and R. A. Hansen (2004), Seismotectonics of the central Denali fault, Alaska, and the 2002 Denali fault earthquake sequence, *Bull. Seismol. Soc. Am.*, *94*, S156–S174.

Reasenberg, P., and D. H. Oppenheimer (1985), FPFIT, FPPLOT AND FPPAGE: Fortran computer programs for calculating and displaying earthquake fault plane solutions, *U.S. Geol. Surv. Open File Rep.*, *OFR-85-739*, 109 pp.

Scholz, C. H., and T. C. Hanks (2004), The strength of the San Andreas fault: A discussion, in *Rheology and Deformation of the Lithosphere at the Continental Margins*, edited by G. D. Karner al., pp. 261–283, Columbia Univ. Press, New York.

Sonder, L. J. (1990), Effects of density contrasts on the orientation of stresses in the lithosphere: Relation to principal stress directions in the Transverse Ranges of California, *Tectonics*, *9*, 761–771.

Weimer, S. (2001), A software package to analyze seismicity: ZMAP, *Seismol. Res. Lett.*, *27*, 373–382.

Zoback, M. D., and G. C. Beroza (1993), Evidence for near-frictionless faulting in the 1989 (M6.9) Loma Prieta, California, earthquake and its aftershocks, *Geology*, *21*, 181–185.

Zoback, M. L. (1992), First- and second-order patterns of stress in the lithosphere: The world stress map project, *J. Geophys. Res.*, *97*(B8), 11,703–11,728.

O. S. Boyd and R. L. Wesson, U.S. Geological Survey, MS 966 Box 25046, 1711 Illinois Street, Golden, CO 80225, USA. (rwesson@usgs.gov)